BEAM COMMISSIONING OF SPALLATION NEUTRON AND MUON SOURCE IN J-PARC

Shin-ichiro Meigo*, Motoki Ohi, Shinichi Sakamoto
and Masatoshi Futakawa, J-PARC JAEA Tokai Ibaraki Japan
Hiroshi Fujimori, J-PARC KEK Ibaraki Japan

Abstract

In J-PARC, the Materials and Life Science Experimental Facility (MLF) is aimed at promoting experiments using the world highest intensity pulsed neutron and muon beams which are produced at a thick mercury target and a thin carbon graphite target by 3-GeV proton beams, respectively. The first beam was delivered to the target without significant beam loss in May 2008. Stable operation with beam power of larger than 300 kW succeeded for 1 hour. In order to confirm stable operation of the facility, especially for the integrity of the target, it is important to obtain the beam profile at the target. We developed a new technique by using an imaging plate which was attached on the front of the target by the remote handling technique.

INTRODUCTION

In the Japan Proton Accelerator Research Complex (J-PARC) [1], a MW-class pulsed neutron source, the Japan Spallation Neutron Source (JSNS) [2], and the Muon Science facility (MUSE) [3] were installed in the Materials and Life Science Experimental Facility (MLF). The 3-GeV proton beam is introduced to the mercury target for a neutron source and to the carbon graphite target of 20-mm thickness for a muon source. In order to utilize the proton beam efficiently for secondary particle productions, both targets are aligned in a cascade scheme, where the graphite target is located 33 m upstream of the mercury target.

The 3-GeV proton beam is delivered from a rapid cycling synchrotron (RCS) to the targets. Before injection to the RCS, the proton beam is accelerated up to 181 MeV by the LINAC. The beam is accumulated in short bunches of less than 600-ns duration and accelerated up to 3 GeV in the RCS. After extraction, the 3-GeV proton beam is introduced to the muon production target and the spallation neutron source by a beam transport system having length of 314 m. In May 2008, the first beam was delivered to the target without significant beam loss. In November 2009, a continuous operation has began with beam power of 120 kW. In December 2009, stable operation with beam power of 300 kW for 1 hour succeeded.

Recently it became evident that pitting damage appears in the vessel of the mercury target [4]. It has been reported that the damage on the mercury target vessel is proportional to the 4th power of the beam peak current density [4]. For the high intensity spallation neutron source, beam properties such as beam profile and peak current density are indispensable. In order to obtain the beam profile on the target in the earliest stage of the beam commissioning, we applied a foil activation technique [7] in which the residual dose distribution was measured on an aluminum foil placed in front of the target placed by human hands. The result given by the foil activation technique showed a good agreement with the result by Multi-Wire Profile Monitor (MWPM). However, it is impossible to perform the same activation technique again because the residual does on the target is extreme high such as several Sv/h. Therefore, a new technique is required to measure the beam profile on the target.

BEAM PROFILE ON THE TARGET

Beam Monitors

In order to observe beam properties, we have developed beam monitors [5, 6]. To measure the beam intensity, Current Transformers (CTs) are installed in the beam line. Inside the current transformers, a titanium duct is attached for connection to other vacuum equipment. To measure the beam position and shape, 15 pieces of Multi-Wire Profile Monitors (MWPMs) are installed in the beam line. Silicon Carbide (SiC) is used as sensor wires due to their small interaction with the primary beam. The wire frame can be moved out so that thbeam can pass without interaction when no measurement is performed. A stationary type of beam profile monitor was located at the proton beam window. The proton beam window is located at 1.8 m upstream of the neutron target, which consists of aluminum alloy ($AlMg_3$) having thickness of 5 mm in total. In order to recognize beam profile on the muon production target, a movable profile monitor is placed. For observation of the beam center position without interaction, we installed 14 pieces of Beam Position Monitors (BPMs) along beam transport line. The position of the beam is measured by the induction of wall currents in a quadruple electrodes. Beam position can be obtained by the difference among the pulse heights of signals generated in the electrode. To know the beam-loss status we installed 200 pieces of beam loss monitors at the front of all quadrupole magnets where the beam diameter becomes relatively large. If the amount of beam loss exceeds a certain level, the beam will be immediately stopped by the Machine Protection System (MPS).

* meigo.shinichiro@jaea.go.jp

Beam Profile Measurement by Imaging Plate

In order to perform beam profile measurement by activation, access to the target is necessary after beam irradiation. The radiation around the target is, however, extremely high such as several Sv/h. Therefore a remote handling technique is required. We have developed an activation technique by utilizing an Imaging Plate (IP). By remote handling technique, an IP (Fuji Film BAS-SR 2040) is attached to the target vessel shown in Fig. 1. The IP placed in a holder was attached to the cell crane in the hot cell of MLF by human hands. At the entrance of the hot cell, radiation dose was less than 1 mSv/h so that human can access. The IP approached to the target by the crane and contacted with the target by help of the master slave manipulator as shown in Fig. 1. Typical duration of exposure time of the IP was 5 min. After the exposure, the radiation image was read out by the reader of the IP.

In Fig. 2, the beam profile result obtained by the IP after 120-kW beam irradiation is shown. In the distribution, it was recognized that a clear Gaussian peak exists without tilting, which showed the similar result by foil activation technique [7]. Figure 2 also shows the horizontal distribution obtained by the IP. The distribution can be well described by the combinations of two Gaussian functions having small and large widths. The shorter width was thought to be the incident protons. The longer one was thought to be the secondary particles mainly neutrons and background exposure which was caused during transfer of the IP around at the target.

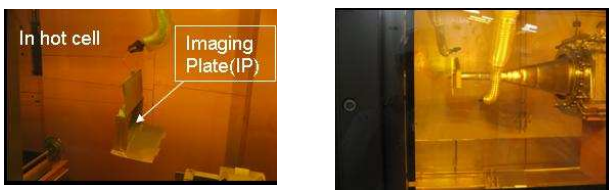

Figure 1: Beam profile measurement using the IP placed on the mercury target vessel by remote handling technique performed after beam irradiation at hot cell. The IP placed in a holder (left) was contacted with the target by help of the master slave manipulator (right).

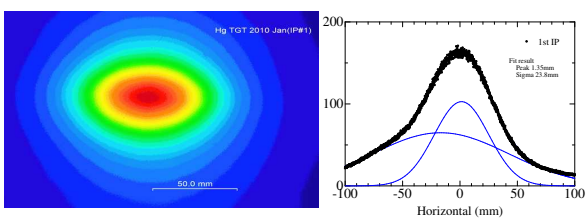

Figure 2: Result of beam profile obtained by the IP. 2D profile (left) and profile on the horizontal axis with the Gaussian fitting curves (right).

Profile Obtained by MWPM

During beam operation, beam profile was continuously measured by the MWPM located on the proton beam window. For each pulse, Gaussian function fitting was performed to obtain peak heat density. Beam profile on the target is slightly different from the profile on the MWPM, because of the beam divergence. In order to obtain the beam profile on the target, the beam width is expanded by about 20% on the MWPM to correct the width for the divergence of the beam.

As the power increased, we expanded gradually the beam size. In each run, it was found that the results obtained by the IP and the MWPM showed good agreement within 5%. Therefore, we can obtain a reliable beam profile on the mercury target from the MWPM. It should be noted that the muon production target is placed in the beam position during long period for users beam supply.

MEASUREMENT OF BEAM OPTICS PARAMETER

Dispersion Function

By changing the momentum, beam position is shifted as the dispersion function. From the shift of the beam position, we tried to obtain the dispersion function. In the measurement, by changing RF in the RCS, the beam momentum was shifted $\pm 0.4\%$ from the nominal momentum of 3 GeV. The dispersion function can be obtained from the shift of beam position divided by the momentum difference. Figure 3 shows the experimental results compared with calculation result. It was found that the design calculation showed a good agreement with the experiment. We designed the dispersion free beam transport line and could demonstrate it.

Transverse Emittance and Twiss Parameter

From the results of the MWPMs, the beam width distribution was obtained. Assuming the beam optics to be designed, we obtained the beam emittance and twiss parameter by fitting the beam width distribution. With free emittance and twiss parameters of α and β, the whole distribution was fitted by the TRANSPORT [9] code.

In Fig. 4, the beam width distribution, which exhibits standard deviation obtained by fitting Gaussian function, is shown for the beam power of 300 kW with horizontal and vertical tunes of the RCS of (6.42, 6.42) having injection painting area of 150 and 100 π mm·mrad for horizontal and vertical directions, respectively. In Table 1, the results of beam emittance in RMS are shown. It was found that, as increase of beam power, the beam emittance increased. This fact is mainly caused by the space charge effect in the accelerator. In Table 1, the result of beam emittance calculation for 300 kW [8] is shown. It is recognized that the calculation gives a good agreement with the experiment. Also twiss parameters obtained by the present method are

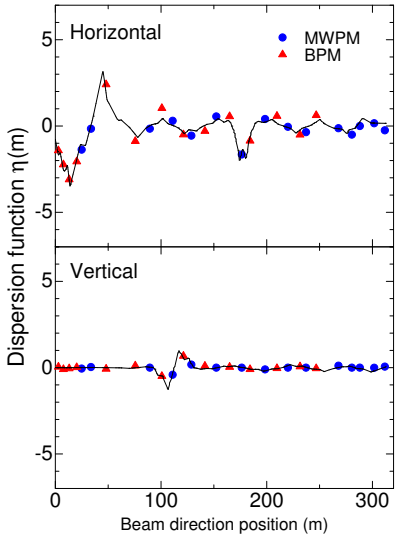

Figure 3: Result of dispersion function obtained by changing momentum of the beam compared with the result of design value.

shown in Table 2. Although slight differences exist, the calculation shows a good agreement with experiment.

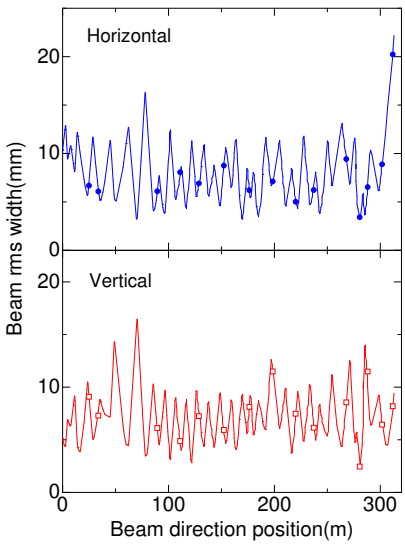

Figure 4: Beam profile measurement for horizontal (top) and vertical (bottom) direction obtained by MWPM and fitting result utilizing free parameter of twiss parameter and emittance.

In beam commissioning, we succeeded in stable operation with beam power of larger than 300 kW. After beam irradiation, the residual dose of radiation on the beam transport line was remarkably small where the highest dose was 20 μSv/h.

Table 1: Beam Emittance (unit: π mm·mrad) Obtained by the Fitting of Beam Width

Beam power (kW)	ϵ_h	ϵ_v	Calculation [8]
120	2.7	2.7	
300	5.3	4.9	5.4

Table 2: Twiss Parameter Obtained by Fitting Beam Width in Horizontal and Vertical Directions for 300 kW Beam

	Experimental		Calculation	
	α	β (m)	α	β (m)
Horizontal	-1.84	20.4	-2.35	24.8
Vertical	0.57	5.28	0.89	5.88

Effect of Muon Production Target

The muon production target causes beam loss. The radiation caused by the muon production target can be measured by the beam loss monitors located several meters upstream of the muon target. In order to observe beam transmission rate, we measured difference of beam intensities by the CT located downstream of the target with and without muon target. It is found that the experimental result of transmission is 93.1% and calculation gives 94.0%. The calculation shows a good agreement with the experiment.

SUMMARY

In order to measure the beam profile on the mercury target, the new technique has been developed utilizing the IP and remote handling technique. The beam profile result obtained by IP is in good agreement with the result by the MWPM. Reliable peak density of the proton beam can be obtained. We have measured beam properties and the effect due to the muon production target. It is found that beam properties show a good agreement with calculations.

REFERENCES

[1] The Joint Project Team of JAERI and KEK, JAERI-Tech 99-56, 1999.

[2] Y. Ikeda, Nucl. Instrum. Meth. **A600**, (2009) 1.

[3] Y. Miyake, et al., Physica B **404** (2009) 957.

[4] M. Futakawa, et al., J. Nucl. Matter. **343** (2005) 70.

[5] S. Meigo, et al., Nucl. Instrum. Meth. **A562**, (2006) 569.

[6] S. Meigo, et al., Nucl. Instrum. Meth. **A600**, (2009) 41.

[7] S. Meigo, et al., Proc. of PAC09, Vancouver, BC, Canada, TU6PFP066 (2009).

[8] H. Hotchi, et al., Proc. of IPAC10, Kyoto, Japan, MOPEC068 (2010).

[9] K. L. Brown, et al., CERN 80-04 (1980).